Supplementary Materials:

Supplementary Figures

Supplementary Figure 1

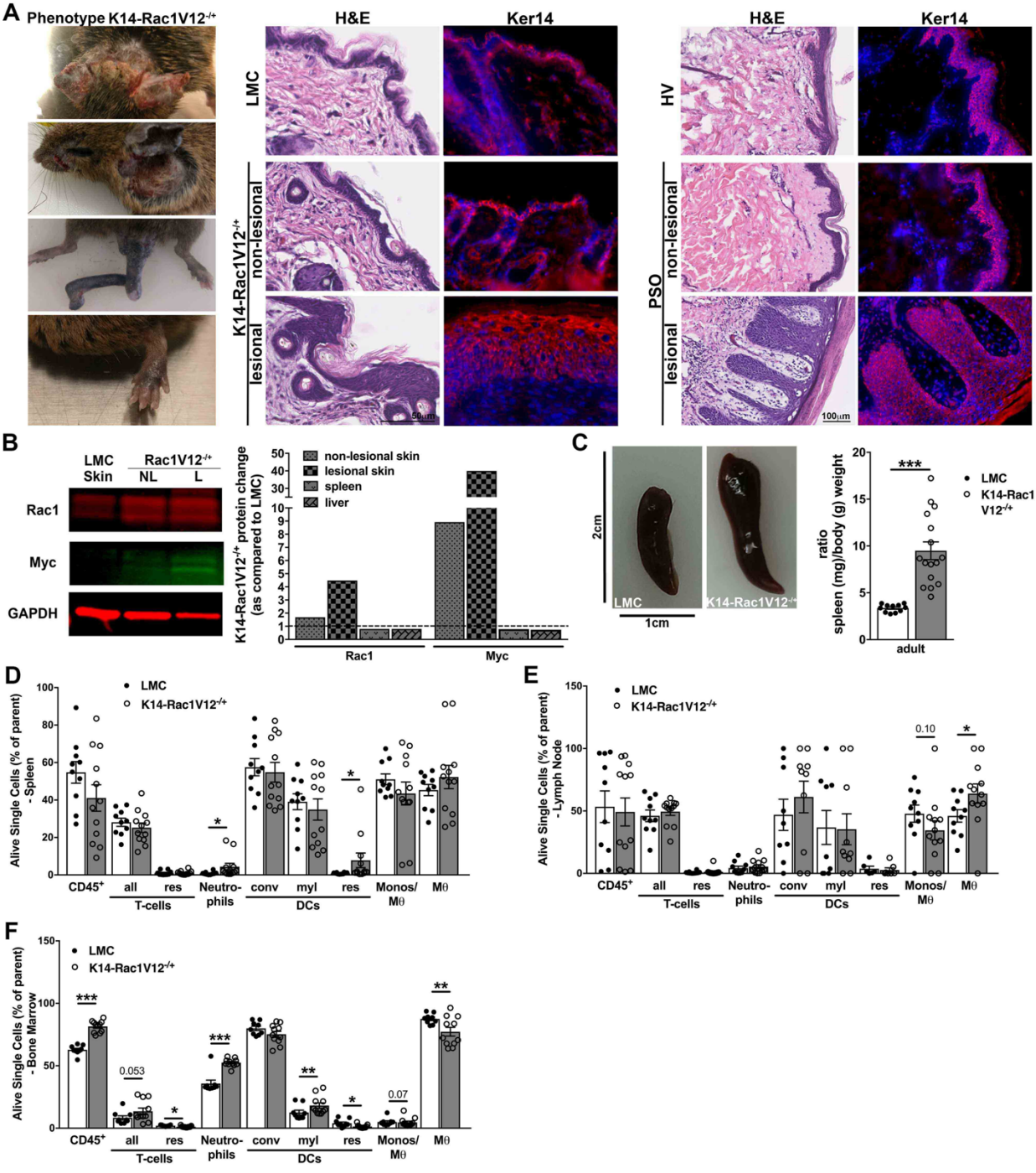

Supplementary Figure 1. Further characterization of the K14-Rac1V12$^{-/+}$ mice and the inflammatory phenotype. (**A**) Keratinocyte exclusive over-expression of the constitutive active mutant of Rac1 V12 in mice resulted in spontaneous psoriasis like lesion development and necrotic shortening of tails of *K14-Rac1V12*$^{-/+}$ mice. Few cases developed one sided limb swelling (left, lower panels). H&E and Cytokeratin 14 staining were performed in mouse and human skin to confirm psoriasis development and comparability of the mouse and human system. (**B**) Western Blot analysis confirmed the exclusive overexpression of Rac1 and the Rac1V12 Myc tag in non-lesional and lesional skin of *K14-Rac1V12*$^{-/+}$ mice while other organs show comparable levels of Rac1 and endogenous Myc between LMC and psoriatic mice. (**C**) Spleens of psoriatic mice are significantly enlarged. (**D-F**) Spleen, lymph node and bone marrow were undertaken flow cytometry analysis to determine and quantify the presence of CD45 positive cells and its subpopulations comparing LMC to *K14-Rac1V12*$^{-/+}$ mice. (Data are expressed as mean ±SEM; n≥10; $p<0.05$ Mann-Whitney test) (LMC-littermate control, HV-healthy volunteer, PSO-psoriasis patient, NL-non lesional, L-lesional, res-resident, DC-dendritic cell, conv-conventional, myl-myleoid, MØ-macrophages)

Supplementary Figure 2

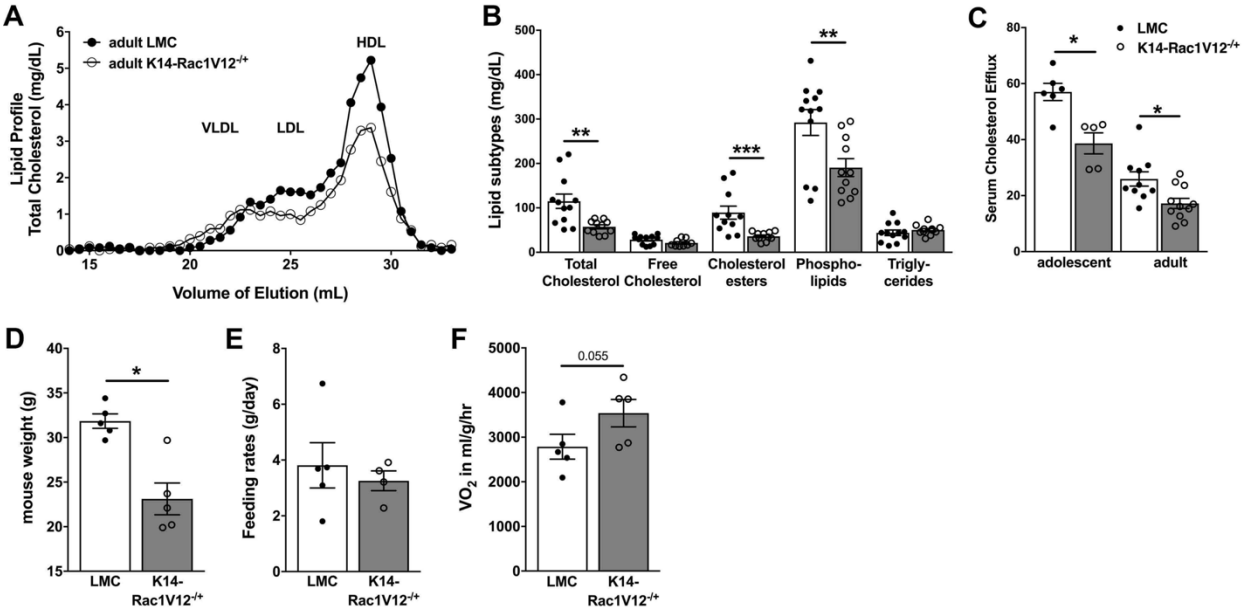

Supplementary Figure 2. Psoriasis-induced inflammation alters the plasma lipid profile. (A) Plasma from fasted age and gender matched mice was used for FPLC-based separation of lipids (n=6/6). **(B)** Whole plasma of fasted mice was used for detailed lipid subtype analysis using ELISA based techniques (n>6/6). (**C**) Functionality of the HDL particle was determined using a cholesterol efflux assay and displayed significant reduction of the psoriatic HDLs capacity accepting cholesterol for reverse cholesterol transport (n≥6/5). (**D-F**) Metabolic parameters of *LMC* and *K14-Rac1V12*$^{-/+}$ mice were determined in special housing cages under controlled feeding conditions (n=5/5). (Data are expressed as mean ±SEM; $p<0.05$ Mann-Whitney test) (LMC-littermate control, VLDL-very low-density lipoprotein, LDL-low-density lipoprotein, HDL-high-density lipoprotein)

Supplementary Figure 3

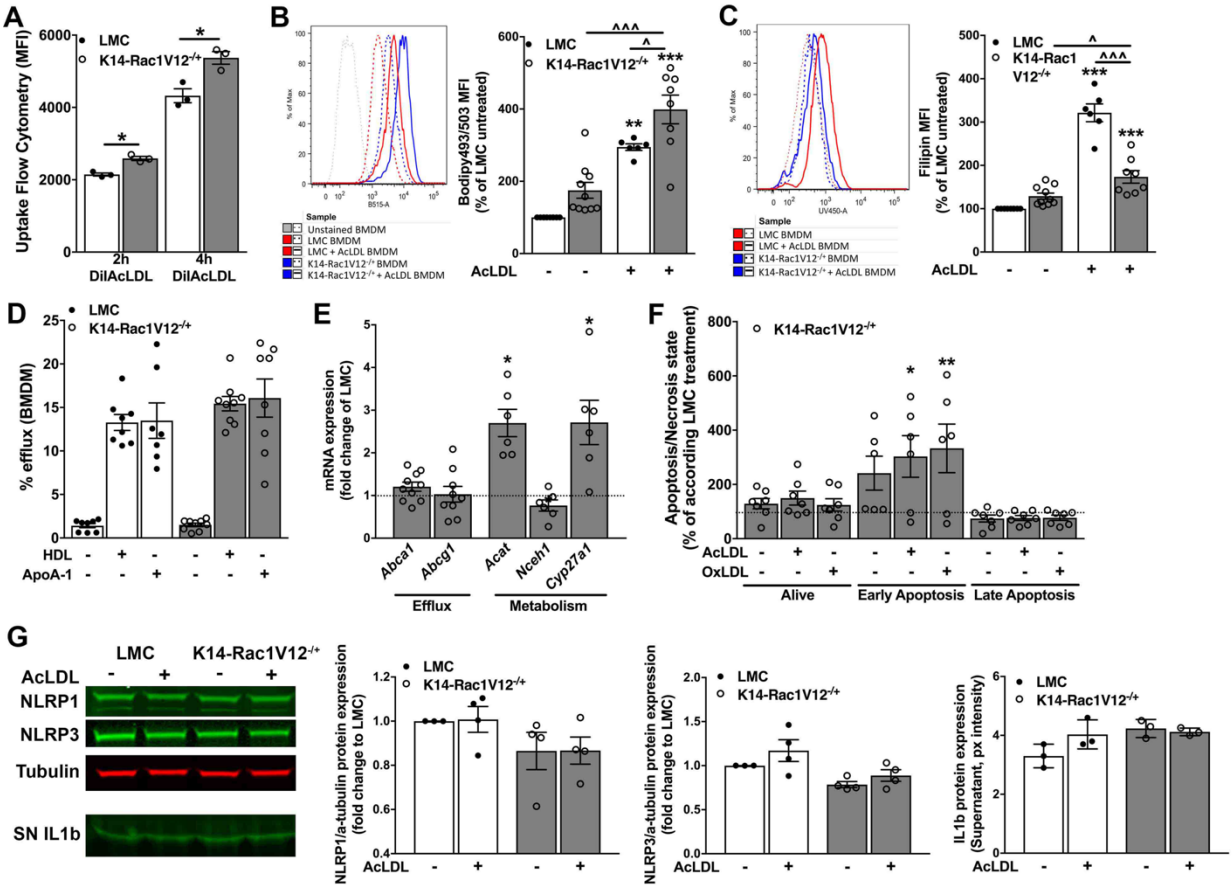

Supplementary Figure 3. Mouse psoriasis macrophages are preprogrammed in a pro-atherosclerotic fashion. (**A**) Modified lipid uptake ability was determined by flow cytometry to confirm fluorescence microscopy findings after treatment with DiI-labeled AcLDL for 2h and 4h (n=3). (**B/C**) Filipin and Bodipy493/503 labeling were used as indicators for cholesterol ester and free cholesterol load of BMDMs analyzed using flow cytometry. A representative histogram blot is shown for each result (n≥6). (**D**) Macrophage cholesterol efflux was determined and revealed no differences between *LMC* and *K14-Rac1V12*$^{-/+}$ mice (n=8). (**E**) RT-PCR analysis was performed to determine possible alterations in cholesterol efflux receptors *Abca1* and *Abcg1* as well as cholesterol metabolism genes (*Acat/Soat, Nceh1, Cyp27a1*) (n≥6). (**F**) Flow cytometry based analysis of annexinV/PI staining of BMDMs revealed increased early apoptotic events in *K14-Rac1V12*$^{-/+}$ macrophages (n=6). (**G**) Further analysis of macrophage cell death showed no

significant differences in NLRP1 or NLRP3 inflammasome activation between the two BMDM groups (n≥3). (Data are expressed as mean ±SEM; n≥6/6; Mann-Whitney test A/E/F $p<0.05$; ANOVA test for B/C/D/G $p<0.017$)

Supplementary Figure 4

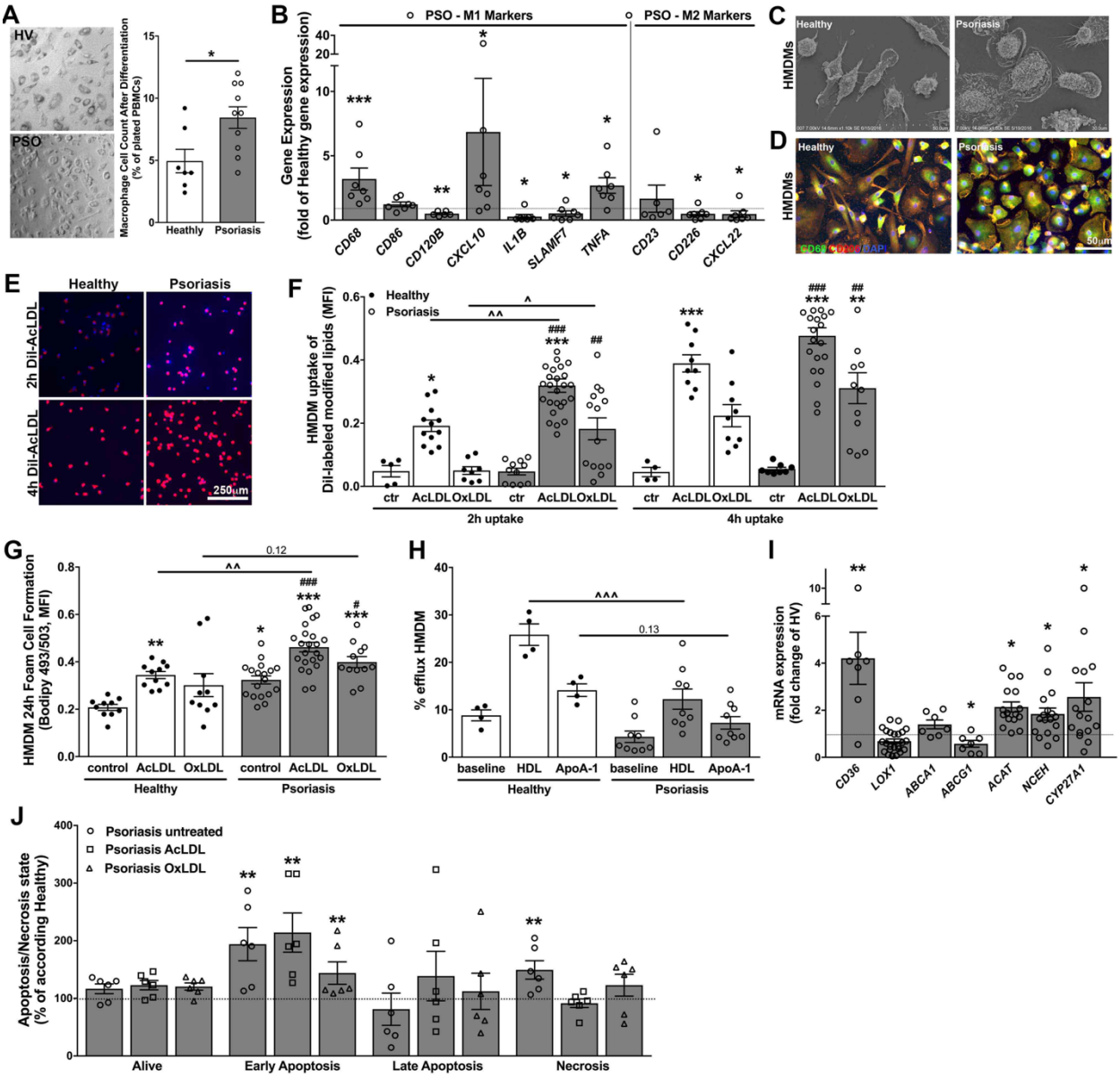

Supplementary Figure 4. Human macrophages isolated from psoriasis patients are preprogrammed in a pro-atherosclerotic fashion. (**A**) Cell count after completed differentiation of human PBMCs into macrophages is increased for psoriatic HMDM. The genetic profile (**B**) is altered in these macrophages as revealed by RT-PCR (nHV/PSO=7/10). (**C**) Scanning electron

microscopy shows shape differences of macrophages from healthy to psoriatic donors (n =3/3). (**D**) Immunofluorescence for CD68 (green) and CD206 (red, nuclei: blue) revealed increased CD68 and decreased CD206 expression in PSO macrophages (n =3/3). (**E, F**) Psoriasis- induced alteration of modified lipid uptake in HMDM was determined by measuring fluorescence intensity per cell of HMDM upon 2h/4h treatment with 20µg/ml DiI-labeled AcLDL or OxLDL (n≥5/8, PSO run in triplicates). (**G**) Macrophage foam cell formation was determined with subsequent Bodipy493/503 labeling (green, nuclei: DAPI, blue) and ImageJ analysis as MFI per cell (n≥5/8, PSO run in triplicates). (**H**) Differences in macrophage cholesterol efflux towards standardized HDL and apoA-1 were determined (n≥4/9). (**I**) RT-PCR technique was used to evaluate possible psoriasis-induced alterations on cholesterol uptake or efflux transporters, and cholesterol metabolism genes in HMDM (n≥4/7). (**J**) Changes in apoptosis and necrosis were determined using AnnexinV/PI staining in flow cytometry (n=3/6). (Data are expressed as mean ±SEM; Mann-Whitney test A/B/I/J $p<0.05$; ANOVA test F/G $p<0.007$, H $p<0.017$; HV-healthy volunteer, PSO-psoriasis; HDL-high-density lipoprotein, LDL-low-density lipoprotein, Ac-acetylated, Ox-oxidized)

Supplementary Figure 5

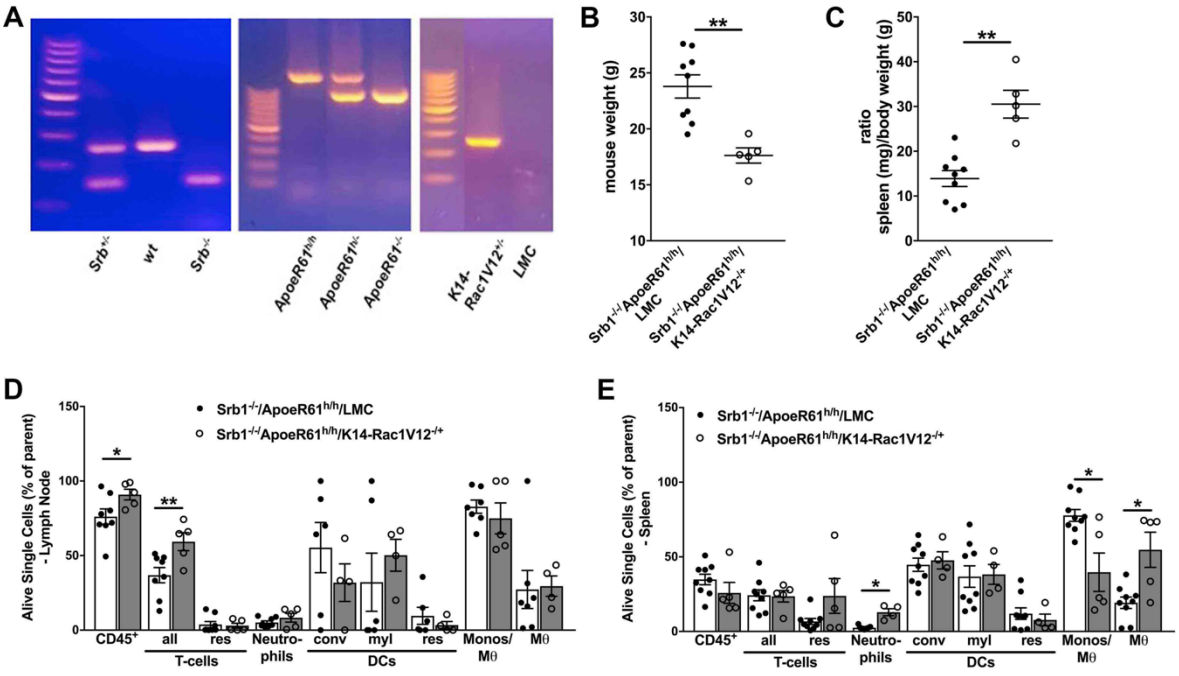

Supplementary Figure 5. Psoriasis increases experimental atherosclerosis in the mouse. (**A**) K14-Rac1V12$^{-/+}$ mice were crossed into atherosclerosis prone SRB$^{-/-}$/ApoeR61$^{H/H}$ mice. Genotyping results with according negative and positive controls as well as possible subtypes are shown. 8-10-week-old female mice with *Srb1$^{-/-}$/ApoeR61$^{H/H}$/LMC* or *Srb1$^{-/-}$/ApoeR61$^{H/H}$/Rac1V12$^{-/+}$* genotype were used for atherosclerosis studies. (**B-G**) Mice were put on HFD for 2 weeks. At sacrifice weight (**B**) and body to spleen weight ratio (**C**) were determined. Using flow cytometry of lymph node (**D**) and spleen (**E**) the cellular composition of these organs was determined. (Data are expressed as mean ±SEM; $p<0.05$ Mann-Whitney test)

Supplementary Figure 6

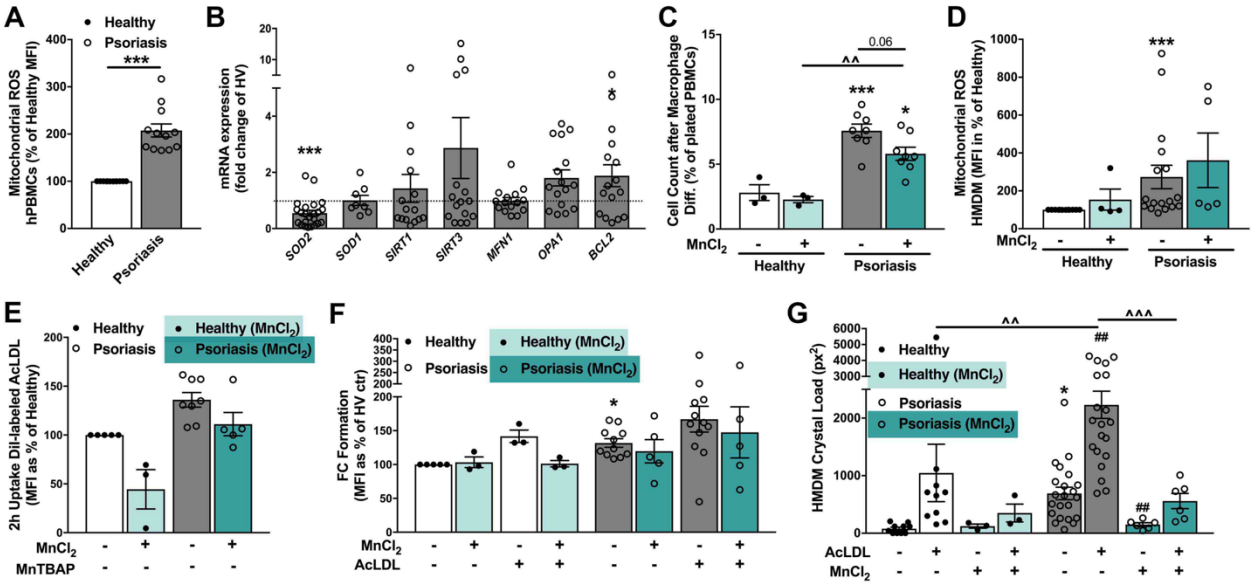

Supplementary Figure 6. SOD2 activity and expression plays an important role in human psoriasis induced macrophage dysfunction. (**A**) Human PBMCs isolated from psoriasis patients display increased mitochondrial ROS using MitoSOX staining and flow cytometry detection. (**B**) Differentiated HMDM show decreased levels of SOD2 mRNA as revealed by RT-PCR (nHV=4, nPSO≥8). (**C**) Differentiation of PBMCs to HMDM in the presence of 5μM $MnCl_2$ was determined (n=3/8). (**D**) Afterwards mitochondrial ROS were detected using MitoSOX labeling and flow cytometry detection (nHV=4, nPSO≥5). (**E**) HMDM lipid uptake was determined by detecting MFIs using ImageJ of control of $MnCl_2$ differentiated HMDM treated with DiI-labeled AcLDL for 2h in control or $MnCl_2$ differentiated macrophages (nHV=3, nPSO≥5). In a similar experimental setup foam cell formation (**F**) was detected upon 24h control or AcLDL treatment and subsequent Bodipy493/503 labeling (nHV=3, nPSO≥5). (**G**) Cholesterol crystal (CC) content was visualized using a polarized light microscope setup and quantified with ImageJ software (nHV≥3, nPSO≥5; PSO run in duplicates). (Data are expressed as mean ±SEM; Mann-Whitney test $p<0.05$ for A/B, ANOVA test for C-G, C/D/E $p<0.017$, F $p<0.01$, G $p<0.008$) (HV-healthy volunteer, PSO-psoriasis patient; Ac-acetylated, LDL-low-density lipoprotein, $MnCl_2$-manganese

chloride, PBMCs-peripheral blood mononuclear cells, FC-foam cell formation, ROS-reactive oxygen species, MFI-median fluorescence intensity)

Supplementary Figure 7

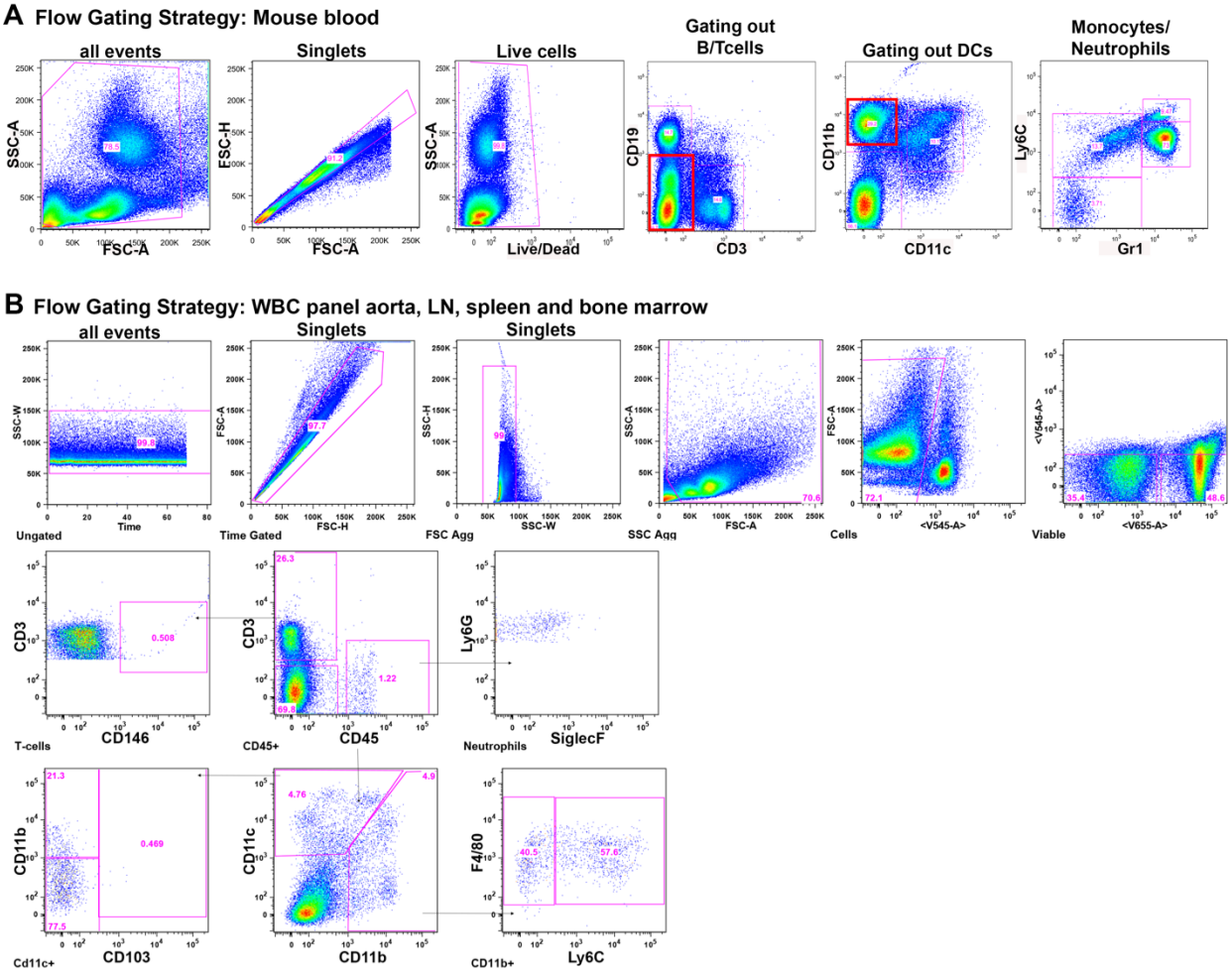

Supplementary Figure 7. Flow Gating Strategies. Flow gating strategies for blood composition flow experiment are shown in (**A**). Flow diagram for analysis of white blood cells within aorta, spleen, lymph node and bone marrow are displayed in (**B**).

Supplementary Tables

Supplementary Table 1: Psoriasis mouse model screening and severity scaling system was based on a 5-point list.

0	Animal with *K14-Rac1V12*$^{-/+}$ genotype but failed to express phenotype
1	Animal with skin lesions on ears or muzzles or tail
2	Animal with skin lesions on ears and/or muzzle and/or tail (2 symptoms must be present)
3	Animal with skin lesions on ears/muzzle/tail and eyes and one of the following: back or head skin or joint swelling
4	Animal with all of the above symptoms
5	Animal from scale 4 with symptoms of fatigue, pain score 3 or lethargy

Supplementary Table 2: Description of antibody cocktail used to determine mouse blood cell composition.

antibody	supplier/Cat#	antibody	supplier
CD3-BV421	Biolegend #100228	CD11c-PE	Biolegend #117308
CD19-PE/Cy7	eBioscience #25-0193-82	CD69-BV605	Biolegend #104530
CD11b-FITC	eBioscience #11-0112-85	F4/80-BUV785	Biolegend #123141
GR-1-PerCp/Cy5.5	Biolegend #108428	Ly6C-APC/Cy7	BD Bioscience #560596
MHCII-eVolve 655	eBioscience #86-5321-42	LIVE/DEAD Aqua	Life Technologies #L34957

Supplementary Table 3*:* Description of antibody cocktail used to determine mouse WBC composition of aorta, lymph node, spleen and bone marrow.

antibody	supplier/Cat#	antibody	supplier
CD45-BV650	BioLegend #103151	Ly6c-PE-cy7	BioLegend #128017
CD11b-eFluor506	eBioscience #69-0112-80	CD146-PerCPcy5.5	BioLegend #134709
CD11c-PE	BioLegend #117307	Ly6g-BUV395	BD #56978
CD103-BV421	BioLegend #121421	CD3-APC Cy7	BioLegend #100221
F4/80-Alexa Fluor647	BioLegend #123121	SiglecF-BV785	BD #740956

Supplementary Table 4: Summary of human and mouse primer pairs used for RT-PCR.

mouse *Gapdh*	F: GGCAAATTCAACGGCACAGT R: CGCTCCTGGAAGATGGTGAT
mouse *Abca1*	F: CCCAGAGCAAAAAGCGACTC R: GGTCATCATCACTTTGGTCCTTG
mouse *Abcg1*	F: CAAGACCCTTTTGAAAGGGATCTC R: GCCAGAATATTCATGAGTGTGGAC
mouse *Cd36*	F: TTGTACCTATACTTGGCTAAATGAGA R: CTTGTGTTTTGAACATTTCTGCTT
mouse *Cd38*	F: AAGATGTTCACCCTGGAGGA R: ACTCCAATGTGGGCAAGAGA
mouse *Fpr2*	F: TCTACCATCTCCAGAGTTCTGTGG R: TTACATCTACCACAATGTGAACTA
mouse *Erg2*	F: TCTACCATCTCCAGAGTTCTGTGG R: TTACATCTACCACAATGTGAACTA
mouse *Cmyc*	F: CCTAGTGCTGCATGAGGAGA R: TCCACAGACACCACATCAATTT
mouse *Arginase1*	F: GGTCTGTGGGGAAAGCCAATGAAGA R: GAGATGCTTCCAACTGCCAGACTGT
mouse *Cd206*	F: CTGCTGCTGAGTCCAGTTTTCTGTC R: AAGCCACTTCCCTTCAACATTTCGG
mouse *Inos*	F: GGAGCCTTTAGACCTCAACAGA R: AAGGTGAGCTGAACGAGGAG
mouse *Tnfa*	F: CTGTAGCCCACGTCGTAGC R: GGTTGTCTTTGAGATCCATGC
mouse *Ifng*	F: ATGAACGCTACACACTGCATC R: CCATCCTTTTGCCAGTTCCTC
mouse *Ldlr*	F: GAAGCCAGGAAAGTGACTCG R: CAGACAGAGGCCCTGAGTTC
mouse *Lox-1*	F: TGGCTATGGGAGAATGGAAC R: GTTGGTTGGGAGACTTTGGA
mouse *Acat/Soat1*	F: GAAAAGGCCAATCTGGAACA R: AGTCTCCTTTCTCCCCCAAA
mouse *Nceh1*	F: AAGTGCTTTACCCCCGAACT R: TGCAGCACTTCAGGATTGTC
mouse *Cyp27a1*	F: GAGAGTGAATCAGGGGACCA R: AGGAAGTGCAGGTAGCCAGA
mouse *Sod2*	F: GCGGTCGTGTAAACCTCAAT R: GCTTGATAGCCTCCAGCAAC
mouse *Sirt3*	F: CTGGGGTGGACACAAGAACT R: CCTGCACTACACCTTCAGCA
mouse *Bcl2*	F: AGCCCGTGTTTGTAATGGAG R: CACAGCCTTGATTTTGCTGA

human *GAPDH*	F: GTCAGTGGTGGACCTGACCT R: AGGGGTCTACATGGCAACTG
human *ABCA1*	F: CTGCTAAGGAGGGAGCCTTT R: AAAAGGGCCACAAACTGTTG
human *ABCG1*	F: CCTACCACAACCCAGCAGAT R: CGGAGTTGCTCAAGACCTTC
human CD36	F: ACGCTTGGCATCTTCAGAAT R: CCCCTGCTCAAGAAACAGAG
human *CD68*	F: TCAGCTTTGGATTCATGCAG R: TGATGAGAGGCAGCAAGATG
human *CD86*	F: CCCTGTAACTCCAGCTCTGC R: AGGCCACCGTTTTCCTTACT
human *CD120b*	F: GGAAACTCAAGCCTGCACTC R: TCCAACTGGAAGAGCGAAGT
human *CXCL10*	F: AGGAACCTCCAGTCTCAGCA R: CCTCTGTGTGGTCCATCCTT
human *IL1β*	F: GGGCCTCAAGGAAAAGAATC R: AGCTGACTGTCCTGGCTGAT
human *SLMF7*	F: GAAGCAGATGCACCTGACAA R: CTGCCTGACTCCAAGTCTCC
human *TNFα*	F: AGCCCATGTTGTAGCAAACC R: GGAAGACCCCTCCCAGATAG
human *CD23*	F: TTCGAGCTGAACAGCAGAGA R: CCATGTCGTCACAGGCATA
human *CD226*	F: ACCTTCTCTCGCAGACCAAA R: GAGAGTGAGGCCAAGACCAG
human *CXCL22*	F: TGTGCCAACTCTCTGCATTC R: AGACCCAGAAGTGGGATGTG
human *SOD2*	F: GCAAGGTGGAACCTTTTGAA R: CGCTGGTCTTGAACTCCTTC
human *SOD1*	F: AGGGCATCATCAATTTCGAG R: GGGCCTCAGACTACATCCAA
human *SIRT1*	F: GCAGATTAGTAGGCGGCTTG R: GCTGGTGGAACAATTCCTGT
human *SIRT3*	F: TCCACATCCCAATTCTGACA R: GAGCTTGCCGTTCAACTAGG
human *MFN-1*	F: CTGGAACCACCAAGGAGTGT R: GCCTCCTGAAGAACAACAGC
human *OPA-1*	F: TCCCGCTTTATGACAGAACC R: GCAAGATAAGCTGGGTGCTC
human *BLC2*	F: GGATGCCTTTGTGGAACTGT R: GGTGCTTGGCAATTAGTGGT
human *LOX-1*	F: GCCATTCCGAAATCAAGAAA R: CTTACCTCTGGGCCACACAT
human *ACAT*	F: TTCAGGGAGCCATTGAAAAG R: CTTCAAGCTTTACCCCACCA

human *NCEH*	F: ACACTGCTCATCTCCGCTTT R: TCTTCCCAGGAGTGAAATGG
human *CYP27A1*	F: AGCTGCGCTTCTTCTTTCAG R: AGCTGGTCCAGTCGAGTCAT
human *LXRα*	F: CGGGCTTCCACTACAATGTT R: TCTCCTGCACAGAGACGATG
human *PPARα*	F: CTGGAAGCTTTGGCTTTACG R: GTTGTGTGACATCCCGACAG
human *SCREBF1*	F: GTGCTTAGCCTCCTGACCTG R: CCCAAGCTGTAGCTCCTGTC
human *SCREBF2*	F: AAGTCTGGCGTTCTGAGGAA R: GAGAGGCACAGGAAGGTGAG

Supplementary Table 5: Summary of primary antibodies and according antigen retrieval methods (AR).

antigen	AR for tissue sections	Supplier
Cytokeratin14	Citrate/heat	AbCam, ab7800, LL002
SM22α	Trypsin at 37°C	Proteintech 10493-1
Moma-2	Trypsin at 37°C	AbCam, ab33451
CD206	n.a.	Novus, NBPI-76296
CD68	n.a.	AbCam, ab955
Rac1	n.a.	AbCam, ab33186
Myc	n.a.	Sigma, C3956